*Anal. Chem.* **2007,** *79,* 5225−5231

# Scanning Electrochemical Microscopy. 58. Application of a Micropipet-Supported ITIES Tip To Detect $Ag^+$ and Study Its Effect on Fibroblast Cells

**Dongping Zhan, Xiao Li, Wei Zhan, Fu-Ren F. Fan, and Allen J. Bard***

*Center of Electrochemistry, Department of Chemistry and Biochemistry, University of Texas at Austin, 1 University Station A5300, Austin, Texas 78712-0165*

**We report the use of a micropipet-supported ITIES (interface between two immiscible electrolyte solutions, also called a liquid/liquid (L/L) or water/oil (W/O) interface) as a scanning electrochemical microscopy (SECM) tip to detect silver ion and explore $Ag^+$ toxicity in living cells. A 1,2-dichloroethane solution containing a commercially available calixarene-based $Ag^+$ ionophore (IV) was injected into a micrometer-size glass pipet to construct an $Ag^+$-selective SECM tip. The local $Ag^+$ concentration, down to the micromolar level, in the vicinity of living fibroblast cells, was monitored by SECM approach curves and through imaging of the uptake and efflux of $Ag^+$ by living fibroblast cells in real time. The results show that several stages of interaction between $Ag^+$ and fibroblast cells exist. Since a number of biological processes of cells are involved with non-redox-active ions, the work presented here provides a new way to explore cell metabolism, drug delivery, and toxicity assessment by SECM.**

Scanning electrochemical microscopy (SECM), most frequently with an ultramicroelectrode (UME) tip (disk diameters, $d \leq 25\ \mu$m), has become a useful scanning probe technique due to its unique ability to explore local chemical activity quantitatively with micrometer or submicrometer spatial resolution.[1] In recent years, SECM has been actively applied by a number of groups to investigate living cells in real time.[2,3] A redox couple is usually used as a mediator, which is sometimes directly involved in the metabolic processes of living cells. Generally, a hydrophobic mediator gives positive feedback, whereas a hydrophilic one gives negative feedback.[4−6] From the magnitude of the positive or negative feedback, the viability of the living cell can be judged. In this application, the choice of the redox mediator is important, because, if the mediator reacts with certain metabolic products of the added drugs, the conclusions drawn may not be correct.[6] Alternatively, one can judge cell viability by a species that is consumed or produced by the cell itself. Oxygen consumption is frequently used for this purpose.[6,7] However, the reduction of oxygen produces hydrogen peroxide at some electrodes, which can be harmful to some cells at a high local concentration. While SECM has been valuable for characterizing living cells by studying electroactive species,[2] an approach that allows electrochemical determination of nonelectroactive species as well, especially at low concentrations, would be useful.

In this paper, we have studied $Ag^+$, which is known to inhibit bacterial and fungal growth,[8] and its effect on a mammalian cell. The mechanisms of the interaction between silver compounds and bacteria are also extensively studied.[9−11] Since silver-containing antibiotics are usually used to deal with wounds, it is important to investigate their toxicity on mammalian epithelial tissue. The effects of various metal ions on mammalian fibroblasts and human tissue mast cells have been tested in vitro.[12−15] Metal ions produce dose-dependent cytopathogenic effects in distinct cell types. The similar response of cells to some heavy metal ions implies that these ions may act on fibroblasts by similar mechanisms. Within 4 h, the rate of metal ion uptake correlates well with the depression of succinic dehydrogenase activity. With longer exposure, ∼8 h, protein synthesis is depressed. Silver ions inhibit the proliferation of human dermal fibroblasts after 24-h exposure mainly through the inhibitory action on DNA synthesis and depletion of intercellular ATP content.[15] Nevertheless, in situ monitoring silver ion in

* To whom correspondence should be addressed. Telephone: (512) 471-3761. Fax: (512) 471-0088. E-mail: ajbard@mail.utexas.edu.

(1) Bard, A. J., Mirkin, M. V., Eds. *Scanning Electrochemical Microscopy*; Marcel Dekker: New York, 2001.
(2) Bard, A. J.; Li, X.; Zhan, W. *Biosens. Bioelectron.* **2006**, *22*, 461−472, and references cited therein.
(3) Amemiya, S.; Guo, J.; Xiong, H.; Gross, D. A. *Anal. Bioanal. Chem.* **2006**, *386*, 458−471.
(4) Liu, B.; Rotenberg, S. A.; Mirkin, M. V. *Anal. Chem.* **2002**, *74*, 6340−6348.
(5) Li, X.; Bard, A. J. Scanning Electrochemical Microscopy of HeLa Cells−Effects of Ferrocene Methanol and Silver Ion. In preparation.
(6) Zhan, D.; Li, X.; Nepomnyashchii, A. B.; Aviles, M. A.; Fan, F.-R. F.; Bard, A. J. SECM Investigation of Silver Ion Toxicity on Living Fibroblast Cells. Unpublished work.
(7) See, e.g.:Yasukawa, T.; Kaya, T.; Matsue, T. *Electroanalysis* **2000**, *12*, 653−659.
(8) Klasen, H. J. *Burns* **2000**, *26*, 131−138.
(9) Russell, A. D.; Hugo, W. B. *Prog. Med. Chem.* **1994**, *31*, 351−371.
(10) Schultz, G.; Sibbald, R. G.; Falanga, V.; Ayello, A.; Dowsett, C.; Harding, K.; Romanelli, M.; Stacey, M.; Teot, L.; Vanscheidt, W. *Repair Regeneration* **2003**, *11*, 1−28.
(11) Trevors, J. T. *Enzyme Microb. Technol.* **1987**, *9*, 331−333.
(12) Schedle, A.; Samorapoompichit, P.; Rausch-Fan, X. H.; Franz, A.; Fuereder, W.; Sperr, W. R.; Sperr, W.; Ellinger, A.; Slavicek, R.; et al. *J. Dent. Res.* **1995**, *74*, 1513−1520.
(13) Wataha, J. C.; Hanks, C. T.; Craig, R. G. *J. Biomed. Mater Res.* **1994**, *28*, 427−433.
(14) Hidalgo, E.; Dominguez, C. *Toxicol. Lett.* **1998**, *98*, 169−179.
(15) Poon, K. M. V.; Burd, A. *Burns* **2004**, *30*, 140−147.

10.1021/ac070318a CCC: $37.00 
Published on Web 06/13/2007

the vicinity of living fibroblast cells can aid our understanding of the mechanism of silver action on mammalian epithelial cells. Recent SECM studies on *Escherichia coli* suggested that $Ag^+$ affects the respiratory chain, with ~60% of the silver ion taken up within the cell and 40% binding to the outer membrane of the bacterium.[16]

While $Ag^+$ is electroactive and can be reduced to Ag metal at a tip, its reduction occurs so easily that other reducible species, like oxygen, can interfere with its determination, especially at low concentrations. While stripping techniques can be applied,[16] it would be useful to have an alternative approach, like that based on ion transfer at the ITIES.[17] Ion transfer and facilitated ion transfer (i.e., an interfacial complexation reaction between ion and ionophore) also results in a current flow and can be detected electrochemically.[18−20] Thus, this approach can be used to investigate charge transfers across a L/L interface of ionic species that are not redox active. The ITIES supported in a micropipet have the advantages of being equivalent to an UME and can be used as a SECM tip to study charge transfer across the ITIES and interfaces that are somewhat analogous to biomembranes.[18,21−25] Since a large number of biochemical processes involve ion transfer across the cell membrane, it is useful to learn what occurs in living cells by detecting the concentration of these ions or by stimulating certain processes to occur by modulating the concentration of corresponding ions. In this paper, a supported water/1,2-dichloroethane (DCE) interface micropipet is employed as a SECM tip to monitor local $Ag^+$ concentration in the vicinity of fibroblast cells. The results show that it is a useful method for exploring the interaction between silver ions and fibroblast cells and cell imaging.

## EXPERIMENTAL SECTION

**Chemicals and Materials.** Calixarene-based silver ionophore (IV)[26] and potassium tetrakis(4-chlorophenyl)borate were purchased from Fluka. $Ag_2SO_4$, bis(triphenylphosphoranylidene)-ammonium chloride, and octyltriethoxysilane were supplied by Aldrich. Bis(triphenylphosphoranylidene) ammonium tetrakis(4-chlorophenyl)borate (BTPPATPBCl) was prepared by the same method reported elsewhere.[27] $Na_2SO_4$, $K_2SO_4$, $MgSO_4$, HEPES, D-glucose, and DCE were obtained from Fisher. All chemicals were reagent grade and used as received. All aqueous solutions were prepared with deionized water (Milli-Q, Millipore Corp.). The organic solution was purified DCE.

The 3T3 MEFs WT fibroblast cells (CRL-2752, *Mus musculus* from mouse embryo), Dulbecco's modified Eagle's medium with l-glutamine, fetal bovine serum, dimethyl sulfoxide, and trypan blue were obtained from ATCC and HEPES-buffered saline solution and trypsin neutralizing solution from Cambrex. Trypsin−EDTA solution was purchased from MP Biomedicals, LLC. All of these solutions were used as received.

**Cell Culture and Preparation.** The fibroblast cells from ATCC were grown and maintained in Dulbecco's modified Eagle's medium with l-glutamine/10% heat-inactivated fetal bovine serum while they adhered to the bottom of the Petri dish. The temperature was maintained at 37.5 °C in a water-jacketed incubator (model 2310, VWR Scientific) with 5% $CO_2$. Since $Ag^+$ was added into the solution for some experiments, the chloride-containing growth medium could not be used in electrochemical measurements to avoid the precipitation of silver chloride at certain chloride concentrations. Before the experiments, the growth culture medium was removed and the dish rinsed several times with chloride-free growth medium[28] (in our experiment: 10 mM HEPES, 10 mM glucose, 75 mM $Na_2SO_4$, 1 mM $MgSO_4$, and 3 mM $K_2SO_4$) and then with 25 mM $Na_2SO_4$ aqueous solution. Finally, 0.5 mL of 0.1 mM $Ag_2SO_4$ was mixed with 2 mL of 25 mM $Na_2SO_4$ and added into the Petri dish for SECM measurements. The tip potential was fixed at −0.5 V (as shown in Figure 2) when SECM experiments were performed.

The procedures of cell culture, cell density evaluation, and viability determination were performed according to the instructions provided by ATCC. The cell viability studies with trypan blue were carried out to compare these with the experimental results obtained by SECM. All of the cell procedures were carried out in a sterile fume hood (Liberty Co.), and then the experimental Petri dish was moved and fixed on the SECM stage.

**Instrumentation.** An Olympus inverted microscope (Olympus Co.) was used to observe the cell coverage and growth status of the fibroblast cells. Micropipets were prepared with a model-2000 laser puller (Sutter Instrument Co.) as described elsewhere.[18] An Olympus microscope was used to examine the quality and measure the diameter of the micropipet. SEM images of fibroblast cells were performed using a LEO 1530 scanning electron microscope (Zeiss/LEO, Oberkochen, Germany) to compare these with the SECM images. All of the electrochemical measurements were performed with a commercial SECM workstation (CH Instrument Co., Austin, TX) with the stage mounted on the inverted microscope.

## RESULTS

**Silver Ion Detection with Micropipet-Supported ITIES Tip.** Employing electrochemistry at an ITIES provides a useful way to construct an amperometric ion sensor. Recently, O'Dwyer and Cunnane described silver ion transfer facilitated by the commercial calixarene-based $Ag^+$ ionophore (IV) across the water/DCE interface.[26] They demonstrated that it provided high selectivity and sensitivity for silver ion detection. To explore the uptake and efflux of silver ion by the fibroblast cells, we applied this approach to a sensor designed for SECM use. Figure 1 shows


(16) Holt, K. B.; Bard, A. J. *Biochemistry* **2005**, *44*, 13214−13223.
(17) Volkov, A. G., Deamer, D. W., Eds. *Liquid-liquid Interfaces. Theory and Methods*; CRC: Boca Raton, FL, 1996.
(18) Zhan, D.; Mao, S.; Zhao, Q.; Chen, Z.; Hu, H.; Jing, P.; Zhang, M.; Zhu, Z.; Shao, Y. *Anal. Chem.* **2004**, *76*, 4128−4136.
(19) Zhan, D.; Yuan, Y.; Xiao, Y.; Wu, B.; Shao, Y. *Electrochim. Acta* **2002**, *47*, 4477−4483.
(20) Zhan, D.; Xiao, Y.; Yuan, Y.; He, Y.; Wua, B.; Shao, Y. *J. Electroanal. Chem.* **2003**, *553*, 43−48.
(21) Solomont, T.; Bard, A. J. *Anal. Chem.* **1995**, *67*, 2787−2790.
(22) Shao, Y.; Mirkin, M. V. *J. Electroanal. Chem.* **1997**, *439*, 137−143.
(23) Amemiya, S.; Bard, A. J. *Anal. Chem.* **2000**, *72*, 4940−4948.
(24) Sun, P.; Zhang, Z.; Gao, Z.; Shao, Y. *Angew. Chem., Int. Ed.* **2002**, *41*, 3445−3448.
(25) Burt, D. P.; Cervera, J.; Mandler, D.; Macpherson, J. V.; Manzanares, J. A.; Unwin, P. R. *Phys. Chem. Chem. Phys.* **2005**, *7*, 2955−2964.
(26) O' Dwyer, P.; Cunnane, V. J. *J. Elecroanal. Chem.* **2005**, *581*, 16−21.
(27) Lee, H. J.; Beriet, C.; Girault, H. H. *J. Electroanal. Chem.* **2002**, *453*, 211−219.
(28) Ghandour, W.; Hubbard, J. A.; Deistung, J.; Hughes, M. N.; Poole, R. K. *Appl. Microbiol. Biotechnol.* **1998**, *28*, 559−565.

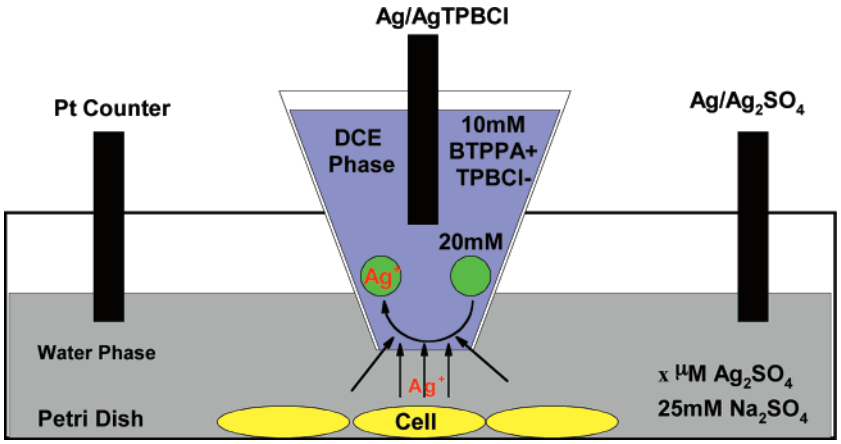


**Figure 1.** Schematic diagram of SECM for the in situ measurement of the local $Ag^+$ concentration in the vicinity of fibroblast cells by using the micropipet-supported water/DCE interface as a tip. Aqueous phase: 20 $\mu$M $Ag_2SO_4$ + 20 mM $Na_2SO_4$. DCE phase: 20 mM silver ionophore + 10 mM BTPPATPBCl.

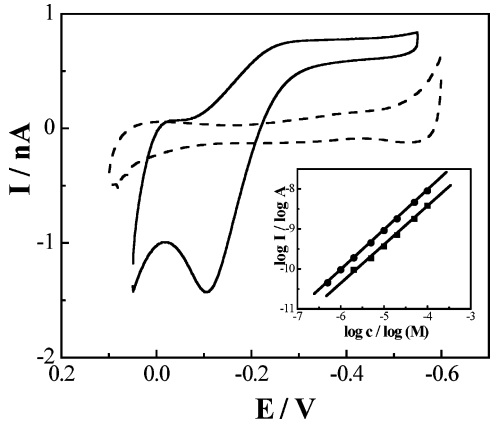


**Figure 2.** Typical voltammograms of the facilitated $Ag^+$ transfer by the commercial ionophore. Radius, *a*, of the micropipet is 18 $\mu$m; the sweep rate is 50 mV/s. The initial potential of the tip was fixed at 0.0 V (no $Ag^+$ transfer) for 6 s and then scanned negatively. The dashed line is the potential window of the system without $Ag^+$ in the aqueous solution. The solid line shows the cyclic voltammogram 3 min after $Ag_2SO_4$ is added into the aqueous solution. The concentration of $Ag_2SO_4$ is 10 $\mu$M. The inset is the linear−log relation between $Ag^+$ concentration, (■) the steady-state current, and (●) the peak current.

the schematic diagram for the detection of silver ions. The micropipet-supported ITIES sensor can be represented as follows:

$$\text{Ag} \mid \text{AgTPBCl} \mid \text{20 mM silver ionophore IV} + \text{10 mM BTPPATPBCl (DCE)} \parallel x\ \mu\text{M } Ag_2SO_4 + \text{20 mM } Na_2SO_4\ \text{(W)} \mid Ag_2SO_4 \mid \text{Ag}$$

Figure 2 shows typical cyclic voltammograms (CVs) of the facilitated $Ag^+$ transfer with the commercial ionophore and a micropipet radius of 18 $\mu$m at a sweep rate, $v$, of 50 mV/s. The dashed line shows the potential window of the system in the absence of $Ag^+$ in the aqueous solution. Then the concentration of $Ag_2SO_4$ in aqueous solution was adjusted to 10 $\mu$M. The cyclic voltammetry was performed from 0.05 V to −0.55 V 3 min after the addition of $Ag_2SO_4$. The solid line shows the CV in the presence of 10 $\mu$M $Ag_2SO_4$ in the aqueous solution. The asymmetric shape of the CV is in accordance with the asymmetric diffusion regime formed at the interface due to the unique shape of the micropipet.[29] When the micro-ITIES was polarized negatively with respect to the $Ag/Ag_2SO_4$ electrode, silver ion was driven into the micropipet and the diffusion field was hemispherical, as depicted in Figure 1. This results in a steady-state current at the micro-W/DCE interface supported at the tip of a micropipet given by[30]

$$I_{ss} = 3.35\pi nFDac \quad (1)$$

where $I_{ss}$ is the steady-state current, $n$ is the charge number of the transferred ion, $F$ is the Faraday constant, $D$ is the diffusion coefficient of the transferred species, $a$ is the radius of the micropipet, and $c$ is the bulk concentration of the ionophore. When the micro-ITIES were polarized positively, the silver ion moved out of the micropipet and the diffusion field became linear, which resulted in a peak current. The peak current is proportional to the concentration of silver ion and the square root of $v$; i.e., the voltammetric behavior follows the Randles-Sevcik equation:

$$i_p = 0.4463 \times 10^{-3}(nF)^{3/2}A(RT)^{-1/2}D^{1/2}cv^{1/2} \quad (2)$$

where $i_p$ is the peak current, $A$ is the area of the micro-ITIES, $R$ is the gas constant, and $T$ is the absolute temperature. From the linear relationship between the current and the concentration of silver ion, both equations give an average diffusion coefficient of $Ag^+$ as $(8.2 \pm 0.4) \times 10^{-6}$ cm$^2$/s. Most importantly, the ionophore shows good selectivity against the alkali, IA, and alkaline earth, IIA, metals that exist in the cells as membrane potential modulators or message transmitters. The supporting electrolyte in this experiment was 25 mM $Na_2SO_4$, which shows no interference in $Ag^+$ detection. The same applies to other IA and IIA cations. Moreover, it does not display a response to many transition metals ions, such as zinc, cadmium, copper, nickel, and iron, which may participate in the processes of cell metabolism. O'Dwyer and Cunnane reported that when these interferents were added as sulfate salts up to 5 × $10^{-5}$ M in the presence of $Ag^+$, the

(29) Stewart, A. A.; Taylor, G.; Girault, H. H.; McAleer, J. *J. Elecroanal. Chem.* **1990**, *296*, 491−515.
(30) Shao, Y.; Mirkin, M. V. *Anal. Chem.* **1998**, *70*, 3155−3161.

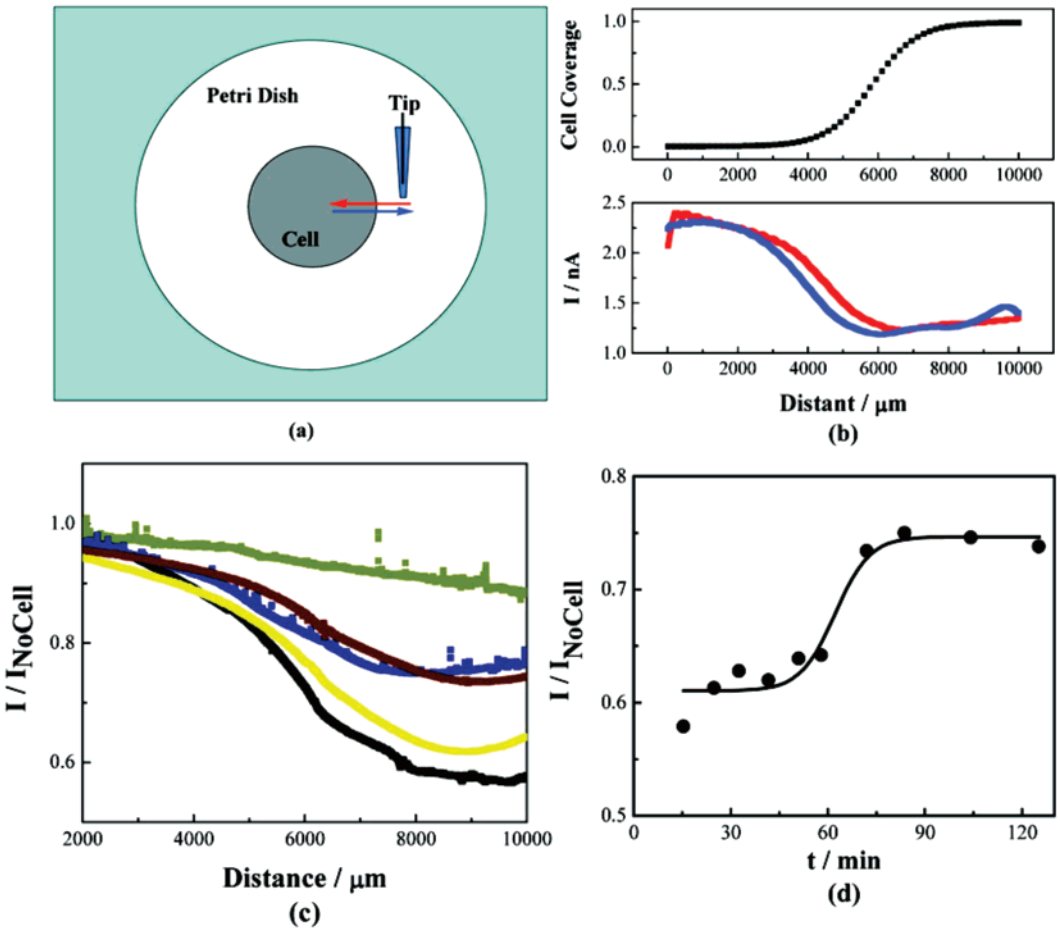


**Figure 3.** $Ag^+$ concentration detected by lateral probe scanning. (a) Schematic diagram of the tip scanning across the region with or without the cell; (b) probe scanning curves from the Petri dish to the fibroblast cell monolayer (the red curve) and the reverse scan (the blue curve), The upper graph shows the sigmoidal fit of cell coverage along the scan line; (c) normalized probe scanning curves recorded at different times after $Ag^+$ addition: 15 (black), 42 (yellow), 84 (navy), 125 (wine), and 210 min (yellow); (d) normalized current changes above the monolayer of the fibroblast cells with exposure time to $Ag^+$ ($x = 9000$ $\mu$m). The tip potential was held at −0.5 V, and the scanning rate was 300 $\mu$m/s.

amperometric response to 0.05 mM $Ag^+$ remained constant throughout.[26] The detection limit, defined as a signal/noise ratio of 3, can reach 1 $\mu$M through the steady-state current and 0.2 $\mu$M through the peak current.

**Lateral Probe Scanning over the Monolayer of Fibroblast Cells.** Investigators chose a monolayer of organisms or certain cells as a convenient way of obtaining representative information.[31] Single, isolated cells, e.g., of bacteria, are often too small (<1 $\mu$m) to be investigated by SECM at the single-cell level. Moreover, cells communicate with each other, so arrays of cells, like biofilms, monolayers, or multilayers, can be more characteristic of fundamental in vivo biological behavior than single cells, especially for tests of drug toxicity. As shown in Figure 3a, a drop of culture medium with the cell density above $1 \times 10^6$/mL was deposited on the Petri dish. In general, it takes ~6−8 h for the fibroblast cells to adhere to the bottom and form a monolayer of fibroblast cells (coverage >90%) in the drop medium. At the edge of the drop, the cell coverage is not homogeneous. Before scanning the probe laterally toward the monolayer of fibroblast cells, an approach curve was taken to determine the distance between the tip of the micropipet and the bottom of the Petri dish over a region containing no cells. The micropipet tip was then withdrawn 30 $\mu$m to perform the lateral probe scanning experiments. As shown in Figure 3b, as the tip was scanned from outside to inside the cell monolayer region, the current of facilitated $Ag^+$ transfer, indicative of the solution $Ag^+$ concentration, gradually decreased to a constant level. By reversing the tip movement, the current gradually increased to its initial value in the region without cells. The current change is related to the cell distribution at the transition region, the cell coverage, the initial concentration of $Ag^+$, and the scanning time. The upper graph in Figure 3b is a sigmoidal fitting curve of the cell coverage (or surface distribution) from data shown at the bottom of Figure 3b, which agrees with the results observed by optical microscopy. Panels c and d in Figure 3 show the change of the normalized current with respect to time. The normalized current is calculated as the ratio of the current above the cell monolayer and that above the dish region containing no cells. To restore the micropipet tip to its initial conditions following an experiment, the tip was withdrawn 300 $\mu$m and cyclic voltammetry was performed from 0.05 to −0.55 V at $v$ of 50 mV/s for several cycles. After that, the current response of the tip recovered to the value given by eqs 1 and 2 within an acceptable error range (±5%). The lateral distribution would gradually become more uniform with time.

(31) See, e.g., Matsui, N.; Kaya, T.; Nagamine, K.; Yasukawa, T.; Shiku, H.; Matsue, T. *Biosens. Bioelectron.* **2006**, *21*, 1202−1209.

**Approach Curve above a Single Fibroblast Cell in a Cell Monolayer.** Studies of the analytical chemistry of single cells benefits from microfabrication and scanning probe techniques.[32] The aim of the investigation of isolated single living cells might be focused on the studies of the functions of some special elements in the cell, such as ion channels and functional proteins and to contrast the behavior with multicell arrays. Moreover, studying single cells allows one to understand more about cell-to-cell variability as well as changes with time and environment. One of our interests here is to explore the concentration change of $Ag^+$ with time over a single cell by positioning a tip above it. For SECM imaging a single living fibroblast cell, the cell density on the substrate was controlled to ensure a coverage of ~85 ± 10%. After cyclic voltammetry, approach curve experiments were carried out to determine the distance between the initial micropipet tip position and the Petri dish bottom (usually adjusted to 30 $\mu$m), and a SECM image was obtained to locate a single living cell for approach curve experiments. Approach curves at different exposure times were recorded as shown in Figure 4a. The boldface black curve is for a cell-free region and agrees well with the SECM theory for an approach to an insulating surface. To avoid the tip touching the substrate and cell, tip travel was stopped when the current reached 80% of that in the bulk solution. The results are similar to those of the earlier lateral probe scanning experiments (shown in Figure 4b); at first the cell is very active and uptakes $Ag^+$ to balance the abrupt potential change of cell membrane. Phenomenologically, the approach curve deviates significantly from the black line and cannot reach the limiting value even at a large $d/a$ value. As time progresses, the approach curves become more and more like the black curve, but still show some differences due to the uptake of $Ag^+$. Finally, positive feedback is observed, which indicates the passive efflux of $Ag^+$ by the fibroblast cell. The inset in Figure 4a shows what happens when the tip penetrates the cell. When the tip touched the cell membrane and penetrated inside the cell, the currents increased to higher and higher levels and then collapsed to zero. This shows that $Ag^+$ concentration inside the cell was higher than outside the cell.

**Scanning Electrochemical Image of Fibroblast Cell.** We have recently applied SECM imaging to characterize cell viability and drug toxicity with a conventional SECM tip[2] and demonstrate here the ability of the micropipet tip to be used for imaging. Although the constant height mode is usually used in SECM, several groups have also employed the constant distance mode.[33–36] The constant distance mode might have the advantage of excluding tip crashes or the deformation of the cell; however, one must be careful to eliminate any contamination of the distance-sensing electrode embodied in the SECM tip. Since we are mainly interested in the response of the whole cell (e.g., viability), the constant height mode seems to be a good choice because of its technical simplicity. Figure 5 shows the cell image using the micropipet-supported ITIES tip. The negative feedback is based on the uptake of $Ag^+$ by the fibroblast cells. Comparing the cell size with that obtained by SEM (the inset in Figure 5), the negative feedback appears to show the nucleus zone of the fibroblast cells. That is quite different from the images based on positive feedback at a metal tip in our previous work,[5,6] in which the cell size obtained by the SECM image was about the same as that of the SEM image.

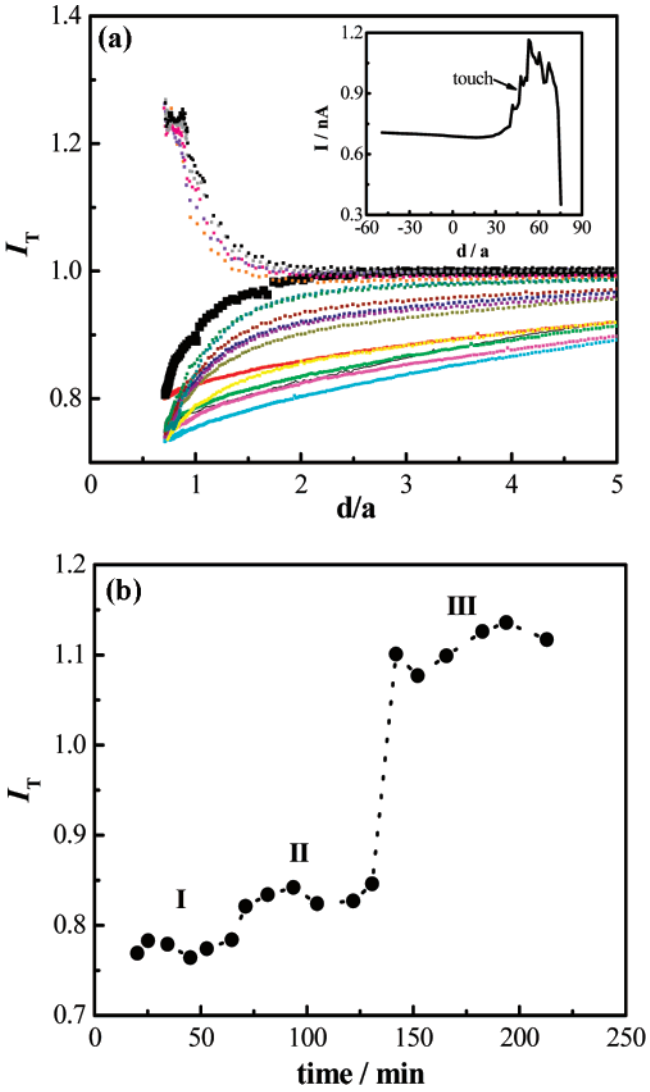


**Figure 4.** (a) Normalized approach curves above a single living fibroblast cell at different times after 40 $\mu$M $Ag^+$ addition. The inset curve shows the process of the tip penetrating the single cell: 20 (red), 25 (green), 34 (yellow), 45 (cyan), 53 (magenta), 65 (dark yellow), 71 (wine), 82 (navy), 94 (purple), 105 (wine), 122 (dark yellow), 131 (royal), 142 (olive), 152 (violet), 166 (orange), 183 (pink), 194 (gray), and 213 min (top black). The negative feedback curve, shown in boldface black, is the approach curve above the Petri dish bottom region without fibroblast cells. The tip potential was held at −0.5 V, and the approach rates were 30 $\mu$m/s. (b) Normalized current changes at $d/a = 1$ with exposure time of $Ag^+$.

## DISCUSSION

When the cells are exposed to an aqueous solution containing micromolar amounts of $Ag^+$, four possibilities of interaction between the cell and $Ag^+$ can be considered: (i) $Ag^+$ can react


(32) Lu, X.; Huang, W.; Wang, Z.; Cheng, J. *Anal. Chim. Acta* **2004**, *510*, 127–138.
(33) Liebetrau, J. M.; Miller, H. M.; Baur, J. E.; Takacs, S. A.; Anupunpisit, V.; Garris, P. A.; Wipf, D. O. *Anal. Chem.* **2003**, *75*, 563–571.
(34) Kurulugama, R. T.; Wipf, D. O.; Takacs, S. A.; Pongmayteegul, S.; Garris, P. A.; Baur, J. E. *Anal. Chem.* **2005**, *77*, 1111–1117.
(35) Borgmann, S.; Radtke, I.; Erichsen, T.; Blöchl, A.; Heumann, R.; Schuhmann, W. *ChemBioChem.* **2006**, *7*, 669–672.
(36) Bauermann, L. P.; Schuhmann, W.; Schulte, A. *Phys. Chem. Chem. Phys.* **2004**, *6*, 4003–4008.

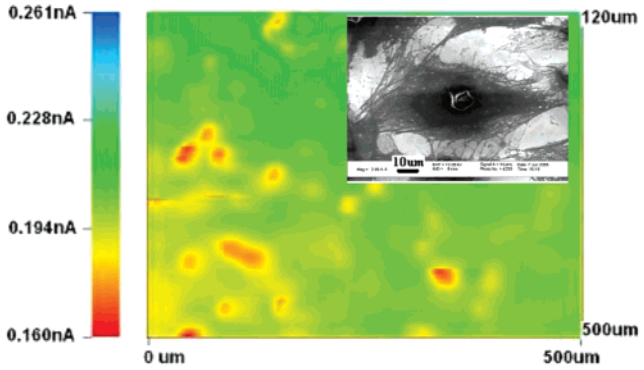


**Figure 5.** SECM image of fibroblast cells recorded at 54 min after exposure to $Ag^+$. The scan rate was 180 $\mu$m/s, and the tip potential was held at −0.5 V. The inset is the SEM image of an individual fibroblast cell in a monolayer. The size of fibroblast cells obtained by SECM images match well to the size of the nuclei obtained by SEM.

with halide anions, $X^-$, and also other anions (e.g., $SO_4^{2-}$) inside the cells to form precipitates on or inside the cell. The halide precipitates can further complex with halide anions and dissolve in the region having high local halide anion concentration.[37] At $[Cl^-] \geq 0.5$ M, significant dissolution of AgCl starts to take place:

$$Ag^+ + X^- \rightarrow AgX\downarrow \quad (3)$$

$$AgX\downarrow + nX^- \rightarrow [AgX_{n+1}]^{n-} \quad (4)$$

$Cl^-$ is an important modulator of cell membrane potential. Although the average intracellular concentration of $Cl^-$ varies from tens to a few hundred millimolar, local $Cl^-$ concentration must be very high especially at the sites of some ion channels (for example, the $Na^+-K^+-Cl^-$ pump).[38,39] (ii) Silver ion can also react with biological ligands, $L_x$, (e.g., DNA, protein) in the cell membrane and inner cytoplasm:

$$Ag^+ + L_x \rightarrow [AgL_x]^+ \quad (5)$$

These ligands usually contain electron donors (e.g., N, O, S) and complex with $Ag^+$. (iii) A ligand-exchange reaction may occur between the small soluble $[AgX_{n+1}]^{n-}$ or insoluble AgX and the bioligands:[40]

$$[AgX_{n+1}]^{n-} + L_x \rightarrow [AgL_x]^+ + (n+1)X^- \quad (6)$$

The ligand-exchange reactions lead to release of halide anions and the formation of new $Ag^+$ complexes. (iv) Since Ag(I) is highly reactive, it can be reduced by certain reductive components in the cell (e.g., hemoglobin[41]) to Ag(0).

$$Ag(I) + e \rightarrow Ag(0) \quad (7)$$

The trapped $Ag^+$ can be reduced to form silver particles in a few hours.[6]

From the results of lateral scanning experiments shown in Figure 3c, three stages of interaction between $Ag^+$ and fibroblast cells can be observed. At the first stage, the fibroblast cells are very active and sensitive to the change of environment. When $Ag^+$ ions are added into the solution, the membrane potential will be disturbed abruptly. To balance the membrane potential, the ion channels are activated and the fibroblast cells take up $Ag^+$. The above trapping processes will enhance the uptake of silver ions by fibroblast cells. The current above the cell monolayer region is 40% lower than that above the dish region without cells, and the lateral concentration gradient can be calculated as 0.4 M/cm (Figure 3b). At the second stage, the current above the cell monolayer region becomes higher and maintains a relatively stable level. We propose that the uptake and efflux of silver ions will slow down and reach a dynamic equilibrium. The complexation reactions between silver ions and ligands could be kinetically slow, since they might involve conformational changes of the biomolecules and reconstruction of the cell membrane. Although the exact mode of interaction between $Ag^+$ and cell is still not clear, $Ag^+$ may uncouple the respiratory chain from oxidative phosphorylation,[42,43] bind to membrane-bound enzymes and proteins containing thiol groups,[44] and interact with intracellular components in cytoplasm.[45] It may also affect the synthesis of DNA. Although the $Ag^+$ concentration above the cell monolayer is lower than that above the dish region without cells, it is still higher than that in the first stage, so the main interaction between the silver ions and cells in this stage is complexation and subsequent chemical reactions. The newly established cell membrane potential is maintained by the influx and efflux of silver ions. At the third stage, the fibroblast cells lose their reactivity and all the processes (uptake, complexation, and efflux) slow down. The lateral concentration gradient from the monolayer of fibroblast cell to the bulk solution tends to be minimized (the top curve in Figure 3c). The result is consistent with our previous results based on oxygen consumption.[6] The respiration of fibroblast cells ceases after ~2-h exposure to 20 $\mu$M $Ag_2SO_4$.

When the micropipet-supported SECM tip was positioned above an individual cell in a cell monolayer, and approached the cell vertically, the results were similar to those of lateral probe scanning during stages I and II. After 2-h exposure to 20 $\mu$M $Ag_2SO_4$, positive feedback was observed. A test with trypan blue showed that more than 40% of the fibroblast cells kept their viability after a 4-h exposure to a solution containing 20 $\mu$M $Ag_2SO_4$ and 20 mM $Na_2SO_4$. Usually a trypan blue experiment overestimates cell life compared to a SECM study,[6] which is in accordance with the comparative results between the fluorescence

(37) Lee, D.; Fortin, C.; Campbell, P. G. C. *Aquat. Toxicol.* **2005**, *75*, 127−135.
(38) Maglova, L. M.; Crowe, W. E.; Smith, P. R.; Altamirano, A. A.; Russell, J. M. *Am. J. Physiol.* **1998**, *275*, C1330−C1341.
(39) Leeves, M. A.; McDonald, F. *Am. J. Orthodon. Dentofac.* **1995**, *107*, 625−632.
(40) Silver, S.; Perry, R. D.; Tynecka, Z.; Kinscherf, T. G. In *Drug Resistance in Bacteria-genetics, Biochemistry and Molecular Biology*; Mitsuhashi, S., Ed.; Japan Scientific Societies: Tokyo, Japan, and Thieme-Stratton: New York, 1982; p 347.
(41) Grier, Nathaniel In *Disinfection Sterilization and Preservation,* 2nd ed.; Block, S. S., Ed.; Lea & Febiger: Philadelphia, PA, 1977; pp 395−407.
(42) Schreurs, W. J.; Rosenberg, H. *J. Bacteriol.* **1982**, *152*, 7−13.
(43) Dibrov, P.; Dzioba, J.; Gosink, K. K.; Hase, C. C. *Antimicrob. Agents Chemother.* **2002**, *46*, 2668−2670.
(44) Zeiri, L.; Bronk, B. V.; Shabtai, Y.; Eichler, J.; Efrima, S. *Appl. Spectrosc.* **2004**, *58*, 33−40.
(45) Feng, Q. L.; Wu, J.; Chen, G. Q.; Cui, F. Z.; Kim, T. N.; Kim, J. O. *J. Biomed. Mater Res.* **2000**, *52*, 662−8.

and SECM image by Kaya et al.[46] One reasonable explanation is that SECM defines cell reactivity, while trypan blue and fluorescence define cell viability. The mark of the complete loss of cell viability is the collapse of the cell membrane. Thus, the SECM positive feedback, as observed with probe scanning, is direct evidence of passive $Ag^+$ efflux. When the micropipet tip approaches the cell and collects $Ag^+$, the local concentration of $Ag^+$ outside the membrane is decreased. The $Ag^+$ inside the fibroblast cell will be released, driven by the change of the cell membrane potential. The case is somewhat similar to the results reported by Liu et al.,[47] where release of dissolved oxygen inside the cell across the membrane was reported to cause positive feedback. The comparative result of the cell size between the SECM images and SEM images indicates that the active region of $Ag^+$ uptake is dominated in the nucleus zone of fibroblast cells.

(46) Kaya, T.; Torisawa, Y.; Oyamatsu, D.; Nishizawa, M.; Matsue, T. *Biosens. Bioelectron.* **2003**, *18*, 1379−1383.
(47) Liu, B.; Cheng, W.; Rotenberg, S. A.; Mirkin, M. V.; *J. Electroanal. Chem.* **2001**, *500*, 590−597.

## ACKNOWLEDGMENT

The support of this work by Nucryst Pharmaceuticals (Wakefield, MA) is gratefully acknowledged.

Received for review February 14, 2007. Accepted May 7, 2007.

AC070318A